**CHEMICAL ENGINEERING TRANSACTIONS** Volume 25, 2011
Editors Jiří Jaromír Klemeš, Petar Sabev Varbanov, Hon Loong Lam
Copyright © 2011, AIDIC Servizi S.r.l., ISBN 978-88-95608-16-7 ISSN 1974-9791
DOI: 10.3303/CET1125119



# Modelling of Calcium Carbonate Synthesis by Gas-Liquid Reaction Using $CO_2$ from Flue Gases

Raluca Isopescu*[1], Mihaela Mihai[1], Constantin Capat[2], Alina Olaru[2], Carmencita Mateescu[3], Ovidiu Dumitrescu[1], Ion Udrea[2]

[1] University Politehnica of Bucharest, Centre of Technology Transfer in the Process Industries
1-5, Gheorghe Polizu Street, Bucharest, Romania, r_isopescu@chim.upb.ro
[2] University of Bucharest, Research Center for Environmental Protection and Waste Management
92, Pandurilor Avenue, Bucharest, Romania
[3] National Institute for Material Physics
105, Atomistilor Street, Magurele, Romania

Green house gases, carbon dioxide, ozone, nitrous oxide and chlorofluorocarbons, result inevitably from fossil fuels combustion. The capture of $CO_2$ from flue gases is an effective way to prevent the threat of global warming. The usage of flue gases with low $CO_2$ content in the synthesis of precipitated calcium carbonate, a valuable mineral compound, seems to be an interesting solution for $CO_2$ permanent removal.
The quality of the solid product obtained (pure polymorphic phase and narrow particle size distribution in micron and sub-micron domain), can increase the value of the process due to the various applications of calcium carbonate (as filler in paper industry, pharmaceuticals, plastic materials and rubber). The present paper analyzes the chemical absorption of $CO_2$ from flue gases in a waste lime solution. The important advantage of this process over conventional technologies of $CO_2$ removal is that it provides a mineral product with many industrial uses, the fine crystallized $CaCO_3$. Based on experimental results a mathematical model including the chemical process and the precipitation of solid phase was developed. The $CO_2$ absorption was modeled using the general model for mass transfer with chemical reaction. The crystallization steps were modeled in the frame of population balance equation. The kinetic parameters corresponding to the crystallization process including nucleation, particle growth and agglomeration were estimated by nonlinear regression using experimental particle size distribution data.

## 1. Experimental study

A 0.5 L bubbling column, made of glass, was used as a gas-liquid contactor. The gas was introduced into the column through the bottom by a 22G3 microporous glass frit. The gas was a mixture of pure $CO_2$ and air, with $CO_2$ concentration varying between 7 and 21 %. Before entering the absorption column, the gas passed through a mixing tube and a humidifier. The gas flow rate was maintained constant in time and measured with a *Cole-Parmer* rotameter. Different gas flow rates were investigated in the range of 125 – 375 L/min. The operation regime in the absorption column was continuous in relation with the gas phase and batch for the absorbent. The liquid phase was prepared in a stirred vessel under inert atmosphere to prevent the possible $CaCO_3$ nucleation by a reaction between the solute and the carbon dioxide present in the laboratory air. The

Please cite this article as: Isopescu R., Mihai M., Capat C., Olaru A., Mateescu C., Dumitrescu O. and Udrea I., 2011, Modelling of calcium carbonate synthesis by gas-liquid reaction using co2 from flue gases, Chemical Engineering Transactions, 25, 713-718
DOI: 10.3303/CET1125119

carbonation solutions simulated the composition of those obtained by the dissolution of $Ca(OH)_2$ from the waste lime. These solutions were prepared from analytical grade $CaCl_2.6H_2O$ and 25% ammonia solution produced by Merck. The resulted pH solutions were in the range 9.5 – 9.7, the molar ratio $Ca^{2+}/NH_3 = 0.5$ and $NH_3/NH_4^+ = 3.0$. A clear solution results after filtration. The pH of solution solutions was in the range 9.5 – 9.7. The initial $Ca^{2+}$ concentration in the liquid was 27 g/L.

The total liquid volume was kept constant during each experimental run. Experiments were carried out at room temperature and under a pressure about 100 kPa. The process was monitored with a pH electrode equipped with a temperature sensor (Ioline, Schott), and a conductivity cell (LF431, Schott) connected to pH/ISE/conductivity measuring instrument (Prolab 4000, Schott). The carbonation process is considered complete when the pH reaches 6.5.

Samples of the liquid phase were withdrawn at certain time intervals to determine the $Ca^{2+}$ concentration with a calcium ion selective electrode (ISE Ca800, W5W) at constant pH. The precipitated calcium carbonate was filtrated, washed with deionized water and dried for 24 hours at $105^0$C. The morphology of the precipitated calcium carbonate was determined from FT-IR spectra using a Perkin Elmer spectrophotometer The particles size distribution was measured by scattering laser beam method.

## 2. Kinetics of absorption process

The overall chemical process of $CO_2$ absorption in a lime solution can be described by the following reactions

1. $CO_2(g) \leftrightarrow CO_2(l)$ (1)

2. $CO_2(l) + OH^- \leftrightarrow HCO_3^-$ (2)

3. $HCO_3^- + OH^- \leftrightarrow CO_3^{2-} + H_2O$ (3)

4. $Ca^{2+} + CO_3^{2-} \rightarrow CaCO_3(aq)$ (4)

5. $CaCO_3(aq) \rightarrow CaCO_3(s)$ (5)

Collier and Hounslow (1999) consider that steps 1 and 5 are very fast. As a result, steps 2, 3 and 4 control the overall rate of reaction. The monitored process data were used to determine the process kinetics. The kinetic rate and equilibrium constants of (2) and (3) process steps that control the overall rate of reaction, were determined by Collier and Hounslow (1999). These constants were used to calculate the supersaturation, S. A set of results is presented in Figure 1. The time evolution of particles size distribution of $CaCO_3$ is presented in Figure 2. This figure reveals that large particles have a small contribution in the product granular structure and that the gas flow rate does not essentially affect the final particle size distribution.

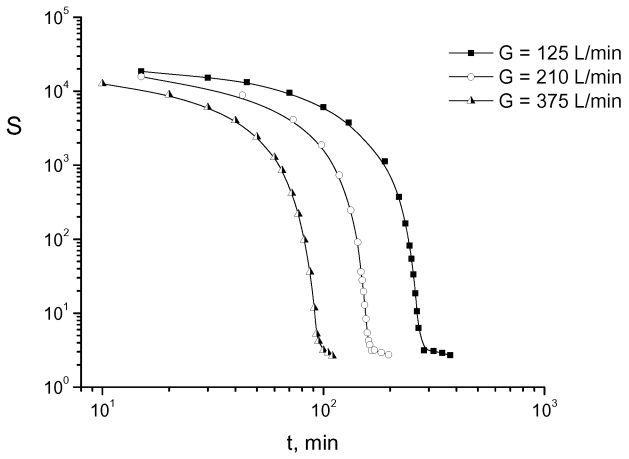


*Figure 1: Time evolution of supersaturation S for different gas flow rates and 12,5 % $CO_2$ concentration.*

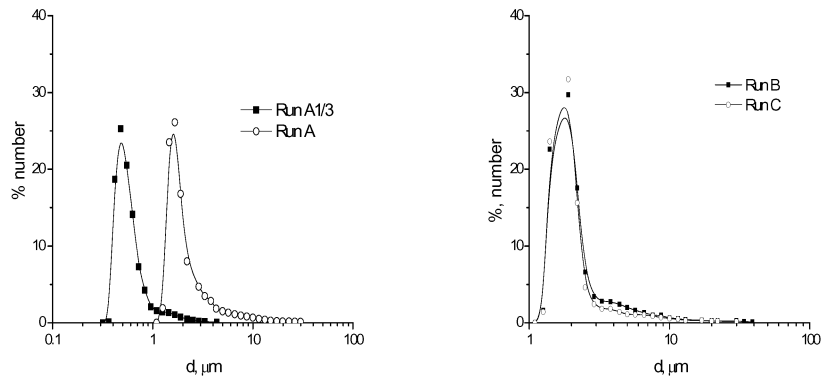


*Figure 2: Particles size distribution of $CaCO_3$ obtained using 12,5 % $CO_2$ concentration and gas flow rate G = 125 L/min after 70 min (run A1/3), 200 min (run A), gas flow rate G=210 L/min (run B), and gas flow rate 375 L/min (run C).*

The morphology of solid phase identified by FT-IR spectra was a mixture of vaterite and calcite. The content of vaterite increased from 85 % (run A) to 93 % (run C) which means that higher rate of supersaturation decrease favor the formation of the less stable polymorph, vaterite.

## 3. Kinetics of precipitation

The mathematical modeling for precipitation process and the kinetic parameter identification was realized in the frame of population balance equation. The analysis of experimental PSD data allow to consider that in calcium carbonate precipitation process nucleation and growth are accompanied by agglomeration. The mechanisms assumed to compete in the solid phase formation were nucleation, size dependent growth and agglomeration. The kinetic parameters that characterize these mechanisms can be estimated by fitting the experimental PSD with the computed values of the particle size distribution. The population balance equation (PBE) that characterizes the precipitation accompanied by agglomeration is represented by an integro-partial differential equation written for a constant suspension volume. This integro-differential equation applied for sparingly salts precipitation can be solved by various methods such as the method of moments, methods of classes (Marshal et al, 1988), using approximation functions (Isopescu and Lavric, 2009). In the present paper the method of classes was chosen and the PBE was transformed into a system of differential equations. Considering $N_i$ the number of particles in unit volume of slurry in class $i$, defined by the characteristic crystal size $L_{i-1}$ and $L_i$, the PBE for class $i$ becomes:

$$\frac{dN_i}{dt} + \left[G(L_i)\cdot n(L_i) - G(L_{i-1})\cdot n(L_{i-1})\right] = B_i + R_{A,i} \tag{6}$$

where $B_i$ is the nucleation contribution in class $i$, $R_{A,i}$ is the agglomeration term. $G(L)$ stands for the size dependent crystal growth rate at size $L$, and $n(L)$ is the population density function. Further we consider that nucleation occurs only in the first class at the nuclei size, so $B_i$ is termed $B_0$ for this class, and is null for all other classes. The nucleation rate was considered to be a function of supersaturation:

$$B_0 = k_B \cdot S^{nb} \tag{7}$$

The classes were defined in a geometric size ration:

$$L_i / L_{i-1} = 2^{1/3} \tag{8}$$

Due to the selected mode of class definition, the agglomeration term may be calculated considering the equation derived by Hounslow et al (1988):

$$R_{A,i} = N_{i-1}\sum_{j=1}^{i-1} 2^{j-i+1}\beta_{i-1,j}N_j + \frac{1}{2}\beta_{i-1,i-1}N_{i-1}^2 - N_i\sum_{j=1}^{i-1} 2^{j-i}\beta_{i,j}N_j - N_i\sum_{j=i}^{nc}\beta_{i,j}N_j \tag{9}$$

For the definition of $G(L)$ the ASL model was selected by defining $G_0$ as the growth rate at minimum particle size:

$$G(L) = G_0 \cdot (1 + a \cdot L)^b \tag{10}$$

As concerning the agglomeration rate, several agglomeration kernels were tested including a size independent form:

$$\beta_{i,j} = \beta_0 \tag{11}$$

The PBE was written for each class and the system of differential equations formed was solved using a Runge-Kutta type method.

The kinetic parameters ($k_B$, $nb$, $G_0$, $a$, $b$, $\beta_0$) were estimated using Luus-Jaakola random optimization procedure to minimize the least squares criterion:

$$F = \sum_i \left[\ln\left(N_{i,\exp}\right) - \ln\left(N_{i,comp}\right)\right]^2 \tag{12}$$

Experimental data analysis reveals a possible change in mechanism during the precipitation. In working condition of run A the supersaturation remains at high levels for about 1/3 of the total reaction time (run A1/3) and then it decreases more rapidly. This fact allows the assumption that nucleation is high in the first period of the reaction and consequently low mean particle sizes and narrow PSD are realized up to 1/3 of the reaction time. The next reaction period seems to be dominated by agglomeration. As a consequence, the integration of the PBE with the same functional form for nucleation and agglomeration gave no good results. The best results were obtained by solving the PBE for the first period of precipitation process, when a large number of nuclei is formed, by considering a size independent agglomeration kernel while for the last period size dependent agglomeration rates had to be considered. An empirical form derived from the differential force kernel (Vanni, 2000) gave the best results. This model may reflect the case in which collisions are originated by motion of particles relative to the fluid in presence of forces acting differently upon the particles. As in the last part of the precipitation process presented in run A, the range of particle sizes increases, and the gas flow rate is moderate, a differential sedimentation can be assumed.

A simplified form is chosen for $\beta_{i,j}$, expressed in terms of class i and j:

$$\beta_{i,j} = \beta_0 \cdot \left(i^{1/3} + j^{1/3}\right)^2 \cdot \left|i^{2/3} - j^{2/3}\right| \tag{13}$$

Alike the differential force kernel, $\beta_{i,j}$ calculated with relation (13) provides a higher probability for efficient collision of small particles with larger ones, explaining the disappearance of very small particles even when nucleation is still important.

The values of estimated kinetic parameters are presented in Table 1.

The kinetic parameters identified prove that the crystallization of $CaCO_3$ is dominated by nucleation and agglomeration. Figure 3 shows that the experimental and computed values for number based distribution are in good agreement.

The long time of the $CO_2$ absorption in the condition of experiment A leads to the formation of larger particles and to the disappearance of small crystals by agglomeration.

*Table 1: Kinetic parameters for precipitation process*

| Period, min | $k_B$, $\#m^{-3}s^{-1}$ | nb, - | $G_0$, $ms^{-1}$ | a, $m^{-1}$ | b, - | $\beta_0$, $m^3s^{-1}$ |
|---|---|---|---|---|---|---|
| 0-70 | $6.04\cdot10^9$ | 1.2 | $6.1\cdot10^{-12}$ | $4.2\cdot10^6$ | 0.31 | $6.16\cdot10^{-16}$ |
| 70-200 | $1.22\cdot10^7$ | 0.82 | $2.8\cdot10^{-11}$ | $1.2\cdot10^7$ | 0.072 | $5.15\cdot10^{-19}$ |

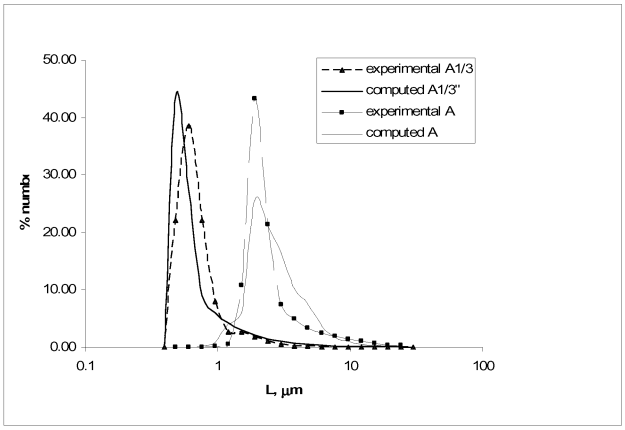


*Figure 3: Experimental and computed number based PSD*

A higher gas flow rate can provide a better mixing and consequently a more rapid decrease of supersaturation. It could also limit the agglomeration effects and thus lead to smaller particle sizes in the final product.

## 4. Conclusions

The present study emphasizes the possibility of using flue gases with low $CO_2$ content to synthesize $CaCO_3$ with small particle sizes. The kinetic parameters identified put into evidence the importance of nucleation and agglomeration in the build up of final particle size distribution. The calculated particle size distribution data are in good agreement with the experiments.

**Acknowledgment:** The authors acknowledge the financial support of research project 22-116 in the frame of National Program II.

## References

Collier A. and Hounslow M., 1999, Growth and Aggregation Rates for calcite and Calcium Oxalate Monohydrate, AIChE Journal, 45, 2298-2305

Hounslow M., Ryall R. L, and Marshall V. R., 1988, A discretized population balance for nucleation, growth and aggregation, AIChEJ, 34, 1821-1832

Isopescu R. and Lavric V., 2009, Kinetic parameters estimation for precipitation using continuous approximation functions and genetic algorithms, Chemical Engineering Transactions, 18, 719-724

Marchal P., David R., Klein J. P. and Villermaux J., 1988, Crystallization and precipitation engineering-I An efficient method for solving population balance in crystallization with agglomeration, Chemical Engineering Science, 43, 59-67

Vanni M., 2000, Approximate Population Balance Equations for Aggregation-Breakage Processes, Journal of Colloid and Interface Science, 221, 143-160